IMPACT OF HEAT AND MASS TRANSFER ON THE UNSTEADY SQUEEZING FLOW OF A NANOFLUID WITH MULTIPLE CONVECTIVE CONDITIONS

A. Sarkar and P. K. Kundu

Dept. of Mathematics, S.A. Jaipuria College, Kolkata, West Bengal, 700005 India
Dept. of Mathematics, Jadavpur University, Kolkata, West Bengal, 700032 India
E-mail: amitformath@gmail.com, kunduprabir@yahoo.co.in

(Received June 9, 2019)

Abstract

In this study, the effect of multiple convective conditions on a viscous unsteady incompressible electrically conductive nanofluid is analyzed. In addition, the fluid is squeezed between two parallel plates in the presence of an applied magnetic field. Nonlinear partial differential equations are remodelled into ordinary ones by introducing similarity transformations, which are solved numerically using the shooting iteration technique together with the Runge–Kutta sixth-order integration scheme; after that, the impact of affined parameters on the temperature and velocity distribution is shown by means of tables and graphs. Our studies suggest that the fluid temperature and the heat transfer rate decrease with the squeeze parameter.

1. Introduction

Studies of heat and mass transfer of a viscous liquid in squeezing drift are important not only for chemical/mechanical engineering (polymer processing, compressing, chemical material loading, and chocolate filtering) but also for our every day life's relevancy. The first study in this context was conducted by Stefan [1]. Mahmood et al. [2] numerically depicted the squeezed Newtonian flow over a porous surface. An axisymmetric and 2D squeezing drift was exhibited by Rashid et al. [3]. Siddiqui et al. [4] addressed the squeezing flow of a magnetic hydrodynamic fluid between infinite parallel plates. Domairry and Aziz [5] analytically extracted a solution for the squeezing flow of a viscous fluid between two parallel disks with blowing. Later, the above work was extended by Hayat et al. [6] to analyze second-grade fluids. Mustafa [7] revealed the squeezing flow of an unsteady viscous liquid. In the presence of Brownian motion, Sheikholeslami et al. [8] analytically (DTM) studied the flow characteristics of a nanofluid drift between two parallel plates. The literature that spotlighted these achievements can be traversed in [9–12].

In the boundary layer drift scenario, two types of conditions—specified surface temperature and specified surface heat flux—are commonly used. It takes place when a linear correlation exists between the surface temperature and the surface heat transfer. Usually, under conditions of Newtonian heating, which is well known as a conjugate convection flow, heat is issued to the convective fluid via the boundary layer with a finite heat capacity. This phenomenon in heat transport rate depends on the local difference in the temperature with the ambient situations. This transcendent aspect of Newtonian heating occurs in many vital engineering devices, such as heat exchanger devices. Relevant studies regarding convective boundary conditions were conducted in [13–16]. Aziz and Khan [17], Das et al. [18], Uddin et al. [19] discussed the convective boundary layer flow of a nanofluid over a convectively heated surface.

The convective heat transfer phenomenon for nanofluid flows over a shrinking sheet was studied by Das et al. [20]. Diversely, in many engineering and technological fields, the solutal boundary condition does a momentous job in the mass transport problems. Tanveer et al. [21] studied the peristaltic flow of a Jeffery nanofluid drift through a curved channel with multiple convective boundary conditions. In that study, they used the mechanism for both heat and mass transfer convective conditions and solved the problem numerically. Recently, multiple convective conditions for non-Newtonian nanofluids have been authorized by Uddin et al. [22]. Later on, Uddin et al. [23] used multiple convective boundary conditions in their study on the free convective dilatant nanofluid flow through a Darcian porous medium. The domination of the second-order slip on nanofluid flow through a permeable sheet was scrutinized by Acharya et al. [24].

In this paper, the foremost objective is to study the aftermath of multiple convective boundary conditions on a squeezing nanofluid flow between two parallel plates. The similarity solutions are derived and used to predict the heat and mass transfer characteristics of the flow. The coordination of the piece is given as follows. Section 2 deals with the mathematical formulation of the flow model. The numerical method and validation of the code are given in Section 3. Results and discussion are presented in Section 4. Conclusions are summarized in Section 5.

2. Mathematical Formulation of the Problem

Consider an unsteady symmetric squeezing nanofluid flow between two parallel plates, as shown in Fig. 1. The fluid is assumed to be incompressible and electrically conducting. In addition, the distance between these plates is $h(t) = H(1 - \alpha t)^{1/2}$, where the plates are squeezed and separated to each other for $\alpha > 0$ and $\alpha < 0$, respectively. Let us consider an unsteady symmetric flow of an incompressible electrically conducting viscous nanofluid between two parallel plates separated by a variable distance $h(t) = H(1 - \alpha t)^{1/2}$, where α is a characteristic parameter having dimensions of time inverse. The upper plate at $y = h(t)$ is approaching the lower stationary plate at $y = 0$ at velocity $v(t)= dh/dt$ until they touch each other, as shown in Fig. 1. A uniform magnetic field of strength $B(t) = B_0(1-\alpha t)^{-1/2}$ (Fig. 1) is adopted perpendicular to the plates where B_0 is the initial intensity of the magnetic field. Here, the electric field is taken as zero. The magnetic Reynolds number is presumed to be small so that the induced magnetic field can be ignored. In the mathematical formulation of the problem, it is supposed that there is no chemical reaction and radiative heat transfer. All body forces are presumed to be ignored. The entire nanofluid structure is in local thermodynamic equilibrium.

Under the stated assumptions, the governing conservation equations in an unsteady state can be expressed as follows [11, 12]:

$$u_x + v_y = 0, \tag{1}$$

$$\rho\left(u_t + u u_x + \mathrm{v} u_y\right) = -p_x + \mu\left(u_{xx} + u_{yy}\right) - \sigma \mathrm{B}^2(\mathrm{t}) u, \tag{2}$$

$$\rho\left(\mathrm{v}_t + u \mathrm{v}_x + \mathrm{v}\mathrm{v}_y\right) = -p_y + \mu\left(\mathrm{v}_{xx} + \mathrm{v}_{yy}\right), \tag{3}$$

$$T_t + uT_x + \mathrm{v}T_y = \frac{k}{\rho C_p}\left(T_{xx} + T_{yy}\right) + \tau\left[D_B\left(C_x T_x + C_y T_y\right) + \frac{D_T}{T_m}\left(T_x^2 + T_y^2\right)\right], \tag{4}$$

$$C_t + uC_x + \mathrm{v}C_y = D_B\left(C_{xx} + C_{yy}\right) + \frac{D_T}{T_m}\left(T_{xx} + T_{yy}\right) \tag{5}$$

where (u,v) signifies the velocity components along the x- and y-axis, respectively; σ characterizes the electrical conductivity; ρ is the density of the nanofluid; μ is the dynamic viscosity; D_B is the Brownian motion coefficient; D_T is the thermophoretic diffusion coefficient; C is the nanoparticle concentration; $\tau=\left(\rho c_p\right)_p/\left(\rho c_p\right)_f$, where $\left(\rho c_p\right)_p$ describes the effective heat capacity of the nanoparticles; T is the temperature of the fluid; T_m is the mean fluid temperature, and κ is the effective heat capacity.

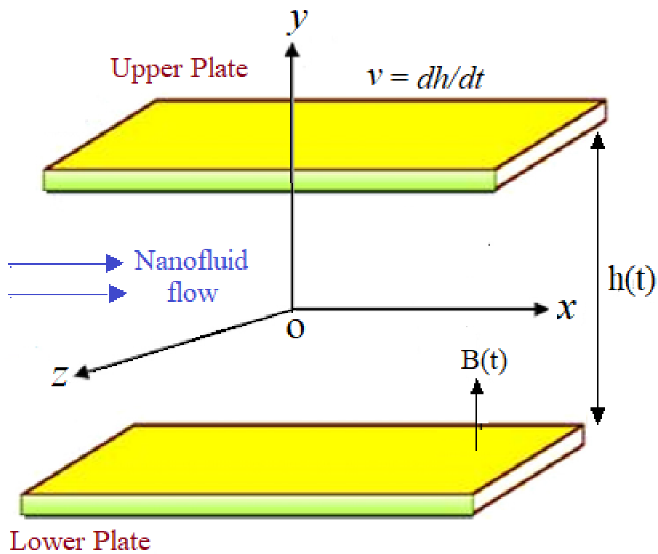

Fig. 1. Geometry of the problem.

The essential boundary conditions for the current study are as follows [11, 12, 24]:

$$\left.\begin{array}{l} u=0, \mathrm{v}=\dfrac{dh}{dt},\ T=T_h, C=C_h \text{ at } y=h(t) \\ u=0,\ \mathrm{v}=0,\ -\kappa\dfrac{\partial T}{\partial y}=h_f\left(T_h-T\right),\ -D_m\dfrac{\partial C}{\partial y}=h_m\left(C_h-C\right) \text{ at } y=0 \end{array}\right\} \tag{6}$$

where T_h and C_h are the temperature and the nanoparticle concentration at the upper plate, respectively. It is assumed that the lower plate is getting hot by means of a hot fluid having temperature T_H and offers the heat transmission coefficient as h_f; D_m stands for the molecular diffusivity of the species concentration; and h_m is the wall mass transfer coefficient.

Using boundary layer approximation and the following similarity transformations:

$$u=\frac{bx}{1-\alpha t}f'(\eta),\ \mathrm{v}=-\sqrt{\frac{b\nu}{1-\alpha t}}f(\eta),\ \theta=\frac{T-T_h}{T_f-T_h},\ \phi=\frac{C-C_h}{C_f-C_h},\ \eta=\sqrt{\frac{b}{\nu(1-\alpha t)}}y \tag{7}$$

equations (1)–(5) reduce to

$$f''''+ff'''-f'\cdot f''-\lambda\left(\eta f'''+3f''\right)-M^2f''=0, \tag{8}$$

$$\theta'' + \Pr(f - \lambda\eta)\theta' + Nb\phi'\theta' + Nt(\theta')^2 = 0 \tag{9}$$

$$\phi'' Nb + LeNb\left(f - \lambda\eta\right)\phi' + Nt\theta'' = 0 \tag{10}$$

with the boundary conditions

$$\left.\begin{aligned} &f(1)=1,\ f'(1)=0,\ \theta(1)=1,\ \phi(1)=0 \\ &f(0)=f'(0)=0,\ \theta'(0)=-\beta_1\left(1-\theta(0)\right),\ \phi'(0)=-\beta_2\left(1-\phi(0)\right) \end{aligned}\right\} \tag{11}$$

Here, $M = HB_0\sqrt{\frac{\sigma}{\mu}}$ is the symbol for Hartmann parameter, $\lambda = \frac{\alpha H^2}{2\nu}$ is the squeeze number, $\beta_1 = \frac{h_f}{\kappa}\sqrt{\frac{\nu}{b}}$ is the thermal Biot number, $\beta_2 = \frac{h_m}{D_m}\sqrt{\frac{\nu}{b}}$ corresponds to the concentration Biot number, $Nt = \frac{\tau D_T\left(T_w - T_h\right)}{\nu T_m}$ represents the thermophoresis parameter, $Nb = \frac{\tau D_B\left(C_w - C_h\right)}{\nu}$ denotes the Brownian motion parameter, $\Pr = \frac{\nu}{\alpha}$ is the Prandtl number, $Le = \frac{\nu}{D_B}$ describes the Lewis number.

The most important characteristics of heat and mass transfer are reduced Nusselt number Nur and reduced Sherwood number Shr, which are defined as follows:

$$Nur = -\theta'(0) \text{ where } Nur = \sqrt{1-\alpha t}\,Nu \tag{12}$$

and

$$Shr = -\phi'(0) \text{ where } Shr = \sqrt{1-\alpha t}\,Sh \tag{13}$$

3. Solution Method

The set of equations (8)–(10) under boundary conditions (11) was solved numerically using a shooting iteration technique together with the Runge–Kutta sixth-order integration scheme. The unspecified primary conditions were assumed and then integrated numerically as an initial valued problem to a given terminal point. Enhancement was made on the values of assumed missing initial conditions by iteratively comparing the calculated value of the dependent variable at the terminal point with its value given there. The computations were performed using a written program based on the symbolic and computational computer language MAPLE.

To ascertain the accuracy of our numerical results, the present study (in absence of thermal radiation) was compared with the study of Muhammad et al. [12]. The values of Nur and Shr were calculated for various Nt values. Excellent agreement was found between these two sets of results, as shown in Table 1. Thus, the use of the present numerical code for the current model was justified.

Table 1. Comparison of Nur and Shr values for different Nt values

N_t	Present work		Muhammad et al. [12]	
	Nur	Shr	Nur	Shr
0.5	2.599805	0.988231	2.5923	0.9901
1.0	1.747822	0.900912	1.7456	0.9020
1.5	1.108564	0.858981	1.1196	0.8615
2.0	1.011226	-	1.0072	-

4. Results and Discussion

To get an insight into the effects of different parameters of practical importance on the flow characteristics, the numerical results are presented graphically in Figs. 2–11 for several sets of values of the pertinent parameters. In the simulation, the following default values of the parameters are considered: Nb = 0.4, Nt = 0.5, β_1 = 0.2, β_2 = 0.15, λ = –0.5, Le = 1.0, M = 0.5, and Pr = 0.7, unless otherwise specified. Figure 2 shows the effect of squeeze number λ on fluid temperature. With an increase in squeeze number λ (absolute value), θ decreases near the boundary layer region. The upshot is perceptible only in a region close to the lower plate, because the curves tend to merge at large distances from the lower plate. It is worth noting that an increase in λ can be associated with a decrease in the kinematic viscosity, an increase in the distance between the plates, and an increase in the velocity at which the plates move. It is observed from Table 2 that an increase in λ (absolute value) results in a decrease in Nur. Thus, the squeeze number λ has a significant effect on heat transfer due to an increased temperature gradient on the lower plate wall. It is evident from Fig. 3 that θ increases with increasing thermal Biot number β_1 in the boundary layer region and it is maximal near the wall region of the lower plate. A stronger convection leads to a higher heat transfer rate and provokes the thermal effect to penetrate deeper into the quiescent fluid, as shown in Table 2. It is also observed that the heat transfer rate at the lower plate increases with increasing β_1 values. It is evident that the thermal Biot number has a strong impact on the heat transfer and enhances it by almost 116% with a change in the thermal Biot number from 0.1 to 0.3. The effects of the parameters controlling the Brownian motion and thermophoresis on temperature distribution are well presented in Figs. 4 and 5 in the presence of surface convection. It is evident from the figures that θ increases in both the Nb and Nt values and the effect is high up to the lower plate region. As both Nb and Nt increase, the thickness of the thermal boundary layer increases, while the curves become less steep near the upper plate region; this fact indicates a decrease in Nur, as evident from Table 2.

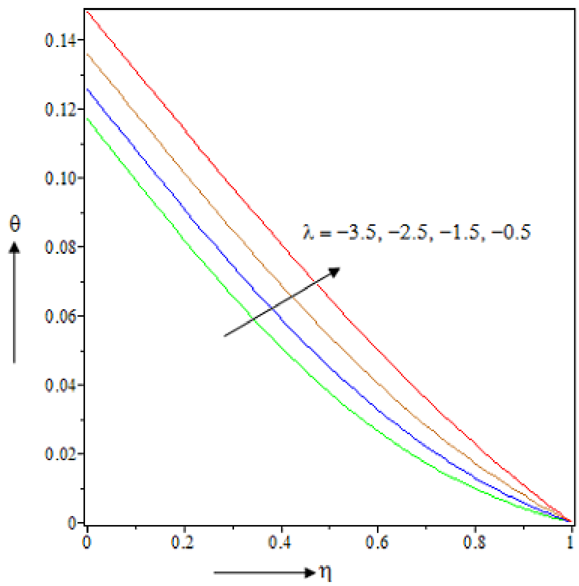

Fig. 2. Concentration profiles for various λ values.

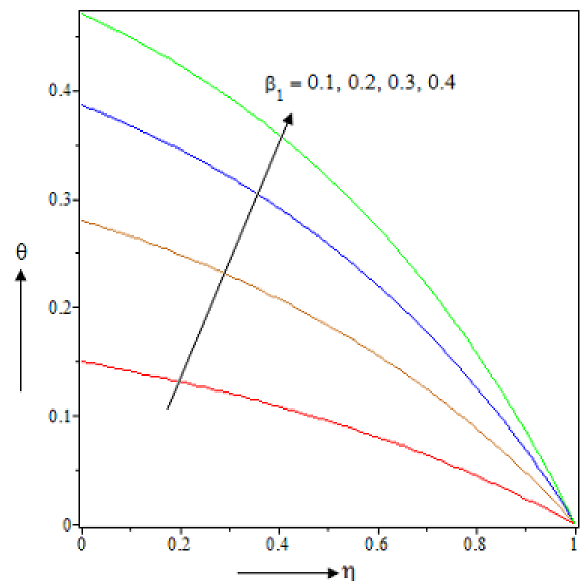

Fig. 3. Concentration profiles for various β_1 values.

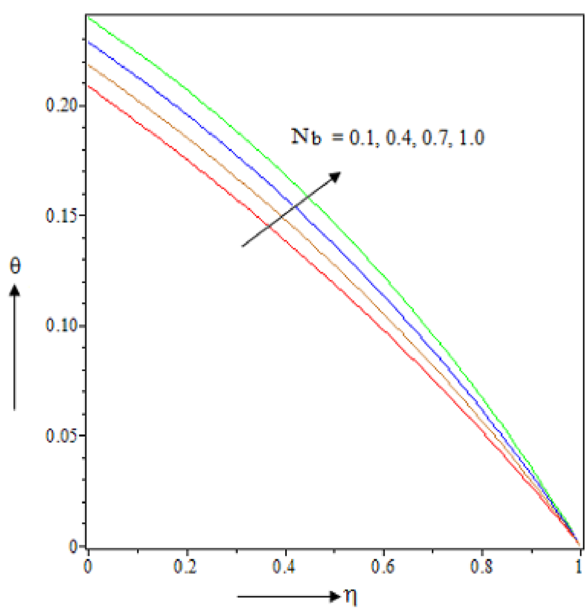

Fig. 4. Concentration profiles for various *Nb* values.

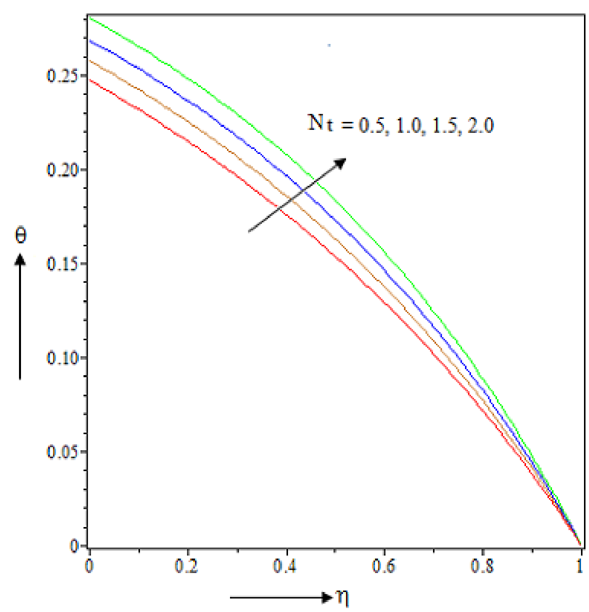

Fig. 5. Concentration profiles for various *Nt* values.

Table 2. Effects of physical parameters on reduced Nusselt number

Nb	*Nt*	β_1	λ	*Nur*
0.1	0.5	0.2	–0.5	0.15827411
0.4	–	–	–	0.15629526
0.7	–	–	–	0.15420971
0.4	0.5	–	–	0.16107681
–	1.0	–	–	0.15957895
–	1.5	–	–	0.15798790
–	0.5	0.1	–	0.08497693
–	–	0.2	–	0.14385373
–	–	0.3	–	0.18389034
–	–	0.2	–1.0	0.16309775
–	–	–	–1.5	0.16197683
–	–	–	–2.0	0.15886899

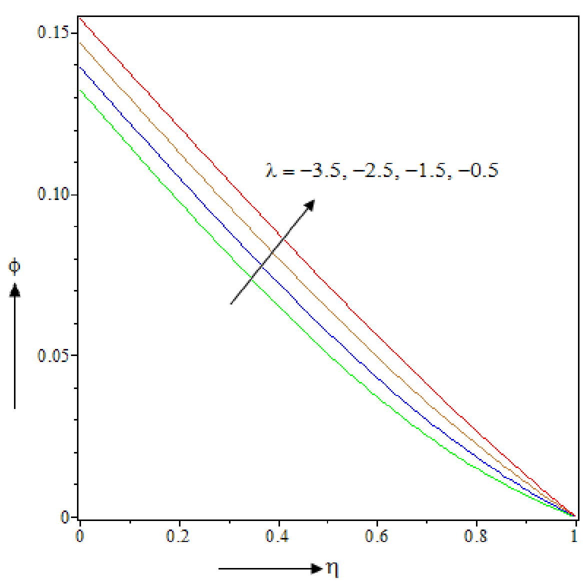

Fig. 6. Concentration profiles for various λ values.

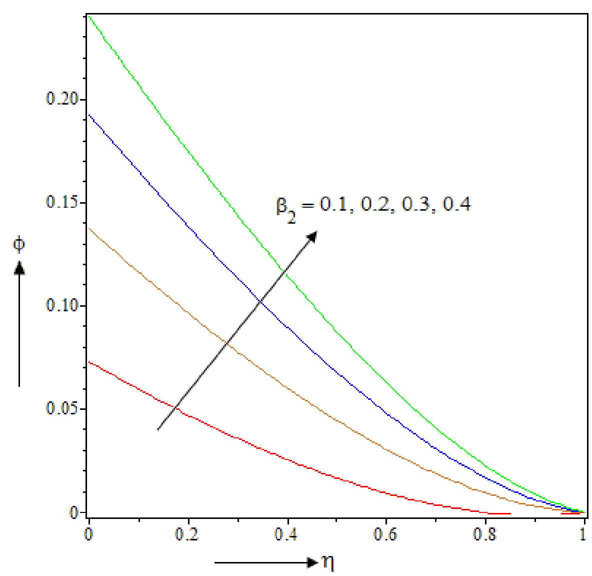

Fig. 7. Concentration profiles for various β_2 values.

With an increase in λ (absolute value), the nanoparticle concentration distribution decreases near the lower plate region, i.e., for $\eta < 0.4$ (not precisely determined); after that, it starts decreasing with an increase in η near the upper plate region, as shown in Fig. 6. It is evident from Table 3 that *Shr* decreases with an increase in λ (absolute value) on the lower plate wall in the presence of surface convection. Figure 7 depicts the variation in the concentration distribution across the boundary layer for different values of concentration Biot number β_2. It is evident that, with an increase in β_2, ϕ significantly increases across the boundary layer near the lower plate. The cause of this trend is that the nanoparticle concentration near the boundary layer becomes wide for larger values of β_2. Further, it follows from Table 3 that Shr increases due to surface convection parameter β_2. Figure 8 reveals that ϕ uniformly increases with increasing Nb values at the squeeze number of $\lambda < 0$. The figure shows that the effect of Nb on the nanoparticle concentration is noticeable only in a region close to the lower plate, as the curves tend to merge at larger distances from the lower plate and, consequently, the concentration boundary layer thickness decreases with increasing Nb. Table 3 shows the effect of Nb on the reduced Sherwood number. It is evident that Shr decreases due to the Brownian motion parameter of nanoparticles. The impact of Nt on ϕ is presented in Fig. 9. It is seen that an increase in the values of the thermophoresis parameter Nt leads to a rapid decrease in the concentration distribution near the lower plate wall region, whereas the concentration decreases gradually from the lower plate region to the upper plate region. It is evident from Table 3 that the thermophoretic effect exerts a strong domination on the mass transfer and enhances it by almost 15.9% with a change in Nt from 0.5 to 1.5.

Table 3. Effect of physical parameters on reduced Sherwood number

Nb	Nt	β_2	λ	Shr
0.1	0.5	0.15	–0.5	0.67302245
0.4	–	–	–	0.43010935
0.7	–	–	–	0.39602982
0.4	0.5	–	–	0.33621418
0.4	1.0	–	–	0.35867916
–	1.5	–	–	0.38970853
–	0.5	0.15	–	0.13297462
-	–	0.25	–	0.20313607
-	–	0.35	–	0.26250404
-	–	0.15	–1.0	0.34039567
-	–	–	–1.5	0.33621418
-	–	–	–2.0	0.33207471

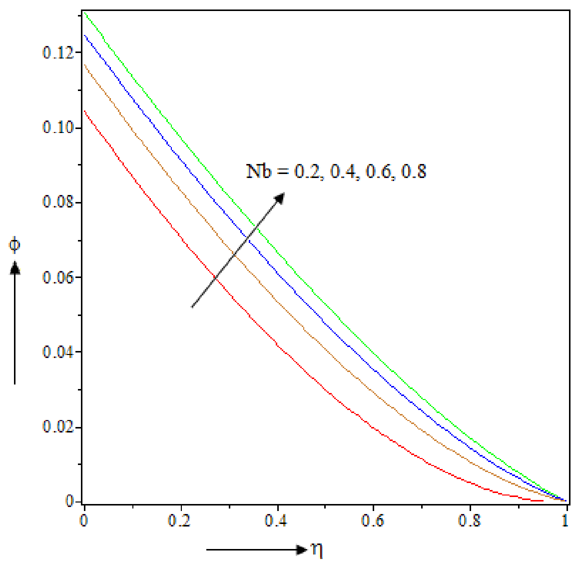

Fig. 8. Concentration profiles for various Nb values.

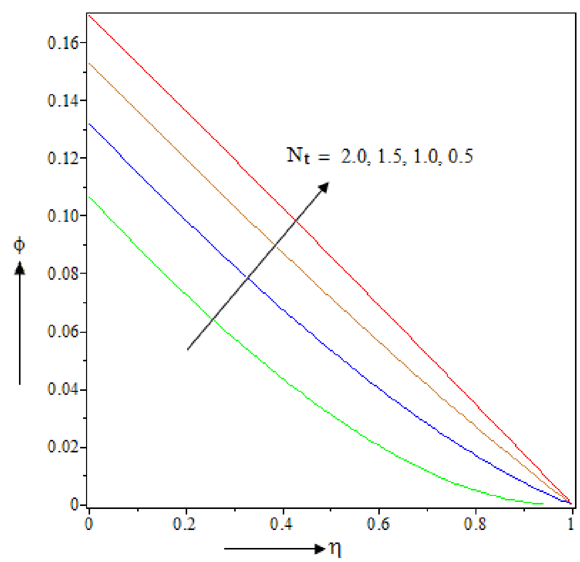

Fig. 9. Concentration profile for various Nt values.

5. Conclusions

In this study, the unsteady squeezing flow in a viscous incompressible electrically conducting nanofluid between two parallel plates is analyzed using a numerical technique. The shooting iteration technique together with the Runge–Kutta sixth-order integration scheme is used to obtain the numerical solution of the nonlinear flow problem. Numerical out-turns are presented through graphs to decorate the details of the heat and mass characteristics and their dependence on material parameters. The use of multiple convective boundary conditions makes the study more general and novel. The results presented here are potentially important for controlling the heat transfer rate and the mass transfer rate. According to the study, some key features are presented as follows:

(i) The Sherwood number at the lower plate decreases with an increase in Brownian motion parameter Nb, squeeze number λ, and Lewis number Le.

(ii) The mass transfer rate vigorously increases due to the occurrence of thermophoresis and surface convection.

(iii) An increase in thermal Biot number β_1 and squeeze number λ leads to an increase in the heat transfer rate at the lower plate.

(iv) It is also observed that, as the Brownian motion intensifies, it affects a larger extent of the fluid and leads to an increase in the thickness of the thermal boundary layer, which in turn decreases the reduced Nusselt number.

Acknowledgments

The authors express their cordial thanks to the respected Editor-in-chief and the honorable reviewer for valuable suggestions and comments to improve the presentation of this manuscript.

References

[1] M.J. Stefan, Abt. II, Österr. Akad. Wiss., Math.-Naturwiss. Kl. 69, 713 (1874).
[2] M. Mahmood, S. Asghar, and M.A. Hossain, Heat Mass Transfer 44, 165 (2007).
[3] M.M. Rashidi, Math. Probl. Eng. 2008, 935095 (2008).
[4] A.M. Siddiqui, S. Irum, and A.R. Ansari, Math. Model. Anal. 13, 565 (2008).
[5] G. Domairry and A. Aziz, Math. Probl. Eng. 2009, 603916 (2009).
[6] T. Haya, A. Yousaf, M. Mustafa, and S. Obaidat, Int. J. Numer. Meth. Fluids 69, 399 (2011).
[7] M. Mustafa, T. Hayat, and S. Obaidat, Meccanica 47, 1581 (2012).
[8] M. Sheikholeslami and D.D. Ganji, Comput. Meth. Appl. Mech. Eng., 283, 651 (2015).
[9] M. Sheikholeslami, D.D. Ganji, and H.R. Ashorynejad, Powder Tech. 239, 259 (2013)..
[10] O. Pourmehran, M. Rahimi-Gorji, M. Gorji-Bandpy, and D.D. Ganji, Alexandria Eng. J. 54, 17 (2015).
[11] N. Acharya, K. Das, and P.K. Kundu, Alexandria Eng. J. 55, 1177 (2016).
[12] S. Muhammad, S.I.A. Shah, G. Ali, M. Ishaq, S.A. Hussain, and H. Ullah, Asian Res. J. Math. 10(1), 1 (2018).
[13] A. Aziz, Commun Nonlinear Sci. Numer. Simul. 14, 1064 (2009)..
[14] O. D. Makinde and A. Aziz, Int. J. Therm. Sci. 49, 1813 (2010).
[15] A. Ishak, Appl. Math. Comput. 217, 837 (2010)..
[16] O.D. Makinde, and A. Aziz, Int. J. Thermal Sci. 50, 1326, (2011)..
[17] A. Aziz and W.A. Khan, Int. J. Therm. Sci. 52, 83 (2012).
[18] K. Das, P.K. Duari, and P.K. Kundu, J. Egypt. Math. Soc. 23(2), 435 (2015)..
[19] M.J. Uddin, O.A. Beg, and I. Md. Ismail, Math. Probl. Eng. 2014, 179172 (2014).
[20] K. Das, N. Acharya, and P.K. Kundu, Appl. Therm. Eng. 103, 38 (2016).
[21] A. Tanveer, T. Hayat, and A. Alsaedi, Neural. Comput. 32(2), 437 (2016).
[22] M.J. Uddin, O.A. Beg, and I. Md. Ismail, Int. J. Numer, Meth. Heat Fluid Flow 26(5), 1526 (2016).
[23] M.J. Uddin, B. Rostami, M.M. Rashid, and P. Rostami, Alexandria Eng. J. 55, 263 (2016).
[24] N. Acharya, K. Das, and P.K. Kundu, Can. J. Phys. 96, 104 (2018).